

ChemComm

Accepted Manuscript



This is an *Accepted Manuscript*, which has been through the Royal Society of Chemistry peer review process and has been accepted for publication.

Accepted Manuscripts are published online shortly after acceptance, before technical editing, formatting and proof reading. Using this free service, authors can make their results available to the community, in citable form, before we publish the edited article. We will replace this *Accepted Manuscript* with the edited and formatted *Advance Article* as soon as it is available.

You can find more information about *Accepted Manuscripts* in the [Information for Authors](#).

Please note that technical editing may introduce minor changes to the text and/or graphics, which may alter content. The journal's standard [Terms & Conditions](#) and the [Ethical guidelines](#) still apply. In no event shall the Royal Society of Chemistry be held responsible for any errors or omissions in this *Accepted Manuscript* or any consequences arising from the use of any information it contains.

COMMUNICATION

A Novel Affibody Bioconjugate for Dual-modality Imaging of Ovarian Cancer

Cite this: DOI: 10.1039/x0xx00000x

Yihong Wang,^{a,b} Zheng Miao,^b Gang Ren,^b Yingding Xu,^b Zhen Cheng^{b*}

An Affibody based dual imaging probe (PET and optical imaging) has been successfully developed. Dendrimer PAMAM G0 was used as a platform to assemble NIRF dye, metal chelator, and Affibody for dual modality imaging of breast cancer. Excellent tumor imaging quality was achieved in both modalities in the living tumor mice models.

Affibody molecules are small nonimmunoglobulin proteins with 58-amino acid residues constituting a three-helix bundle scaffold structure. They can be easily prepared by chemical synthesis for a variety of applications. Some of the advantages of Affibody include high affinity and specificity, rapid blood clearance, excellent tumor penetration and accumulation, and a relatively short *in vivo* half-life.¹ Affibody can be readily labelled with various radioisotopes, near infrared fluorescent (NIRF) dyes, nanoparticles for molecular imaging of tumor biomarkers.² A number of Affibody molecules have been discovered for binding with different tumor targets including epidermal growth factor receptor (EGFR) and human epidermal growth factor receptor 2 (HER2). HER2 is a transmembrane protein and a member of the erbB family of cell surface receptor tyrosine kinase. As a well-established tumor biomarker, it is one of the most important receptors overexpressed in numerous cancer subtypes such as breast, ovarian, lung, gastric, and oral cancers.³ Therefore, imaging of HER2 expression using novel molecular imaging techniques is of great importance to cancer early detection, therapeutic intervention guidance, prognosis of patient survival, and prediction of the response to antineoplastic therapy.

Recently multimodality molecular imaging techniques are becoming more and more important to visualize physiological or pathological of diseases. It takes advantage of strengths of each modality and provides complementary information of diseases that cannot be obtained from a single imaging modality.⁴ Numerous research efforts have been spent to design and develop multimodality probes. In this work, a novel Affibody based dual imaging probe was developed for NIRF and positron emission tomography (PET) imaging of HER2 positive tumors. Such a probe combining both optical and PET offers a robust and reliable imaging capability of both deep and superficial tumor tissues, and it also provides high detection sensitivity and self-confirmation through comparison of two imaging modalities.

A variety of chemical platforms have been used to construct dual imaging probes. Dendrimers are the molecules characterized by repetitive branching patterns. Among the vast dendrimeric family, poly(amido amine) (PAMAM) dendrimers have been studied extensively for various medical applications. The high number of peripheral amine groups, easy tailor, and lack of immunogenicity all make the PAMAM dendrimers well suited for drug delivery, solubility enhancement, imaging contrast agents, neutron capture

therapy, and gene therapy.⁵ In the current study, we chose the smallest PAMAM generation 0 (PAMAM G0) as the core chemical platform, anti-HER2 Affibody Ac-Cys-Z_{HER2:342} as the targeting molecule, along with both NIRF dye Cy5.5 and metal chelator 1,4,7,10-tetraazacyclododecane-1,4,7,10-tetraacetic acid (DOTA) labelled with ⁶⁴Cu as dual reporting moieties to construct a novel dual-modality probe (named as ⁶⁴Cu-DOTA-PAMAM G0(Cy5.5)-Z_{HER2:342}, abbreviated as ⁶⁴Cu-DPCZ, Figure 1).

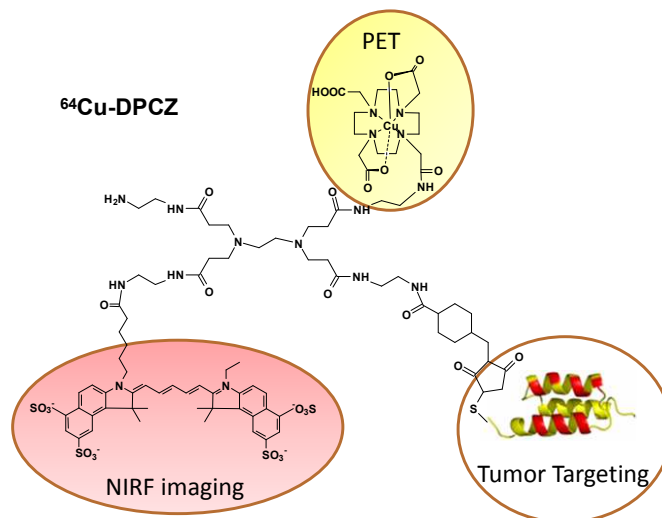


Fig. 1 Schematic structure of ⁶⁴Cu-DPCZ which is constitute by four components, PAMAM G0 as a scaffold, Cy5.5 as an optical reporter, ⁶⁴Cu-DOTA as a PET reporter and Affibody as a tumor targeting molecule.

Synthesis of DPCZ was achieved in four steps (see ESI for details). The PAMAM G0 molecule contains four peripheral amines and can thus accommodates four functional groups via the formation of acylamide. The reporting moieties, Cy5.5-NHS and 2,2',2''-(10-(2-(2,5-dioxypyrrrolidin-1-yl)oxy)-2-oxoethyl)-1,4,7,10-tetraazacyclododecane-1,4,7-triyl) triacetic acid (DOTA-NHS) could be sequentially coupled with primary amines in high yields (>47%) to produce DOTA-PAMAM G0(Cy5.5). A bifunctional linker, sulfo succinimidyl-4-(N-maleimidomethyl) cyclohexane-1-carboxylate (Sulfo-SMCC), was then used to react with an amine group in G0 in a weak base condition. At last, the thiol-reactive maleimide group in Sulfo-SMCC was successfully coupled with the cysteine in Ac-Cys-Z_{HER2:342} in weak acid to form bioconjugate DPCZ (Figure 1). All the products were verified by mass spectrum analysis (MALDI-TOF-MS), and it was confirmed that one Cy5.5, DOTA and Affibody present on PAMAM G0.

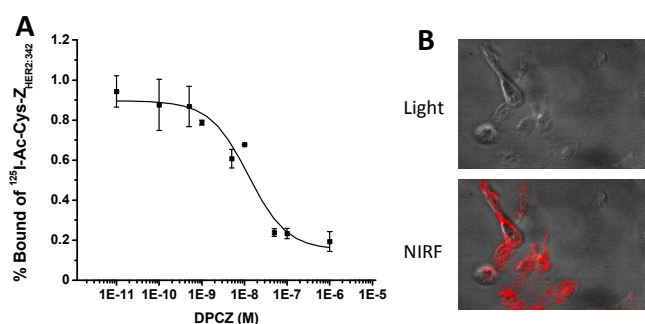


Fig. 2 (A) *In vitro* inhibition of ^{125}I -Ac-Cys- $\text{Z}_{\text{HER2:342}}$ binding to HER2 on SKOV3 ovarian cancer cells by DPCZ ($\text{IC}_{50} = 12.3 \pm 5.5 \text{ nmol/L}$). Results expressed as percentage of binding are mean of triplicate measurement \pm standard deviation. (B) Light (top panel) and fluorescence (bottom panel) images of SKOV3 cells incubated with 1 nM DPCZ for 2 h at 37 °C.

To determine the binding affinity of DPCZ synthesized, Ac-Cys- $\text{Z}_{\text{HER2:342}}$ was first radioiodinated with ^{125}I using the conventional Iodogen method, and the cell binding assay of the resulting ^{125}I -Ac-Cys- $\text{Z}_{\text{HER2:342}}$ was performed using HER2 positive SKOV3 ovarian cancer cell line and DPCZ as a competitor. The study revealed a dose-dependent inhibition of binding of ^{125}I -Ac-Cys- $\text{Z}_{\text{HER2:342}}$ to SKOV3 cells in the presence of DPCZ (concentrations ranging from 10^{-11} to 10^{-6} mol/L) (Figure 2A). The 50% inhibitory concentration (IC_{50}) was calculated to be $12.3 \pm 5.5 \text{ nM}$, which highlighted the high and specific binding ability between DPCZ and HER2-positive cells. Therefore, Affibody conjugated with DOTA-PAMAM G0(Cy5.5) still showed good bioactivity, and the resulting DPCZ was worthy of further biological evaluations. We then performed the *in vitro* fluorescence staining of SKOV3 cells using DPCZ (Figure 2B). Intensive fluorescent signal from SKOV3 cell membrane and intracellular compartments were clearly observed, suggesting that DPCZ can bind with cells and then was internalized. Furthermore, in the presence of unlabeled Ac-Cys- $\text{Z}_{\text{HER2:342}}$ (10 time excess), background fluorescence signal was observed. Again, this result was consistent with the finding from binding affinity study and indicated the specific *in vitro* targeting ability of DPCZ.

The conjugate DPCZ was then labelled with ^{64}Cu to yield ^{64}Cu -DPCZ for realizing PET capability besides of NIRF imaging. ^{64}Cu -DPCZ was intravenously injected into nude mice bearing subcutaneous SKOV3 tumors ($n=3$). At 0.1, 1, 2, 4, 8, and 20 h post-injection (p.i.), the mice were imaged with optical imaging and PET sequentially (Figure 3). Figure 3A and B show typical NIRF and PET images of nude mice bearing subcutaneous SKOV3 tumor after intravenous injection of the ^{64}Cu -DPCZ ($\sim 56 \mu\text{Ci}/6.7 \text{ nmol}$), respectively. From both NIRF and PET images, tumor uptake could be clearly observed as early as at 1 h p.i., and good tumor imaging contrasts were found for all the time points investigated. Interestingly, NIRF imaging revealed that tumor uptake gradually increased with time (Figure 3A), whereas PET images showed that tumor signals increased from 1 to 4 h and then slightly reduced at 20 h. This observation could be explained by the fact that NIRF and PET are following the fate of different reporting moieties (Cy5.5 vs. ^{64}Cu). It has been found that ^{64}Cu -DOTA is not very stable *in vivo* at late time points p.i.⁶ The reduction of Cu(II) to Cu(I) has been considered as the major source responsible for the instability. The macrocyclic polyamines chelation systems including DOTA is unsuitable for Cu(I) species, and transchelation between ^{64}Cu -DOTA and proteins such as serum albumin and superoxide dismutase thus occur. This instability of ^{64}Cu -DPCZ could reduce the probe tumor accumulation. Therefore, novel ^{64}Cu chelation

systems which can stabilize both Cu(II) and Cu(I) species could be used to improve the metal-chelate stability and subsequently circumvent this problem. For example, cross-bridged cyclam ligands or Sar analogues can significantly reduce transchelation and show high *in vivo* stability, and they are good candidates as chelation systems for our future studies.⁷ NIRF imaging also showed that prominent signals from kidneys could be observed, which is consistence with the well documented high kidney uptake of Affibody based probes. Meanwhile, high liver uptakes were shown in PET images (Figure 3B) whereas could not be clearly observed from NIRF images (Figure 3A). This is likely caused by the relatively deeper position of liver located in the mice and high background absorption excitation and emission lights of liver tissue. Further ex vivo NIRF imaging of dissected mice organs and *in vivo* biodistribution studies revealed that ^{64}Cu -DPCZ accumulates in both liver and kidneys, suggesting the clearance through both hepatobiliary and kidney systems (Figure S3).

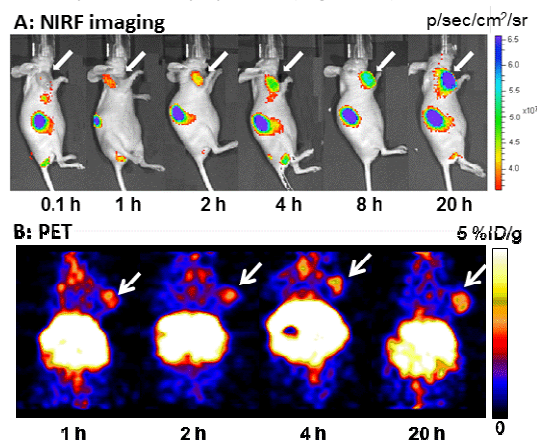


Fig. 3 Dual-modality imaging of ^{64}Cu -DPCZ. (A) *In vivo* NIRF imaging of SKOV3 tumor-bearing mice at 0.1, 1, 2, 4, 8, and 20 h after tail vein injection of ^{64}Cu -DPCZ. (B) Decay-corrected coronal micro-PET images of mice bearing SKOV3 tumor at 1, 2, 4 and 20 h after tail vein injection of ^{64}Cu -DPCZ. Arrows indicate the location of the tumors ($n=3$).

A good imaging probe should possess a number of desirable characteristics such as high tumor uptake, rapid accumulation, and fast clearance. High binding affinity is also among the most important factors. In our research, the dual-modality imaging probe ^{64}Cu -DPCZ that consisted of DOTA, Cy5.5, and $\text{Z}_{\text{HER2:342}}$ with G0 PAMAM dendrimer as the platform was synthesized successfully and employed both *in vitro* and *in vivo*. ^{64}Cu was selected as the radioisotope because of its wide availability, low cost and versatile chemistry. In addition, its E_{max} of 656 keV for positron emission can produce a good spatial resolution in PET images.⁶ Many chelators have been investigated for ^{64}Cu labelling and among those studies, DOTA has been widely used.^{6,7} One of the advantages of DOTA is that it is a universal chelator which can complex a wide variety of imaging and therapeutic radionuclides, although the *in vivo* stability of ^{64}Cu -DOTA complexes has been considered to be moderate. Affibody molecules are small affinity proteins that have been applied in therapeutic, diagnostic, and biotechnological applications.¹⁻³ Affibody $\text{Z}_{\text{HER2:342}}$ was integrated into the probe design via the reaction between thiol group from the Affibody molecule and maleimide from the SMCC moiety. According to the competition assay, IC_{50} of DPCZ was measured to be 12.3 nM. Although lower than the binding affinity of unmodified $\text{Z}_{\text{HER2:342}}$ (22-35 pM) or modified DOTA- $\text{Z}_{\text{HER2:342}}$ -pep2 (65 pM),⁸ DPCZ still maintain viable *in vitro* binding affinity in SKOV3 cells. Further *in vivo* PET and NIRF imaging demonstrated a rapid localization in SKOV3 tumors, good tumor uptake and retention. SKOV3 tumors

could be clearly visualized by both PET and NIRF with good image quality as early as 1 h p.i. Higher levels of tumor-to-normal tissue contrast were achieved at later time points. All these biological evaluation indicate the promise usefulness of the dual probe developed.

A succinct discussion of dendrimer is also warranted here because it is utilized as the platform for construction of ^{64}Cu -DPCZ. Applications of biocompatible dendrimers have been an active area of cancer research in recent years. The particular architecture, flexibility in modifications, and the capability of multiple conjugations to form various hybrids all make dendrimers well suited to serve as a platform for the development of an effective drug delivery device/imaging agent. PAMAM was chosen as the carrier of ^{64}Cu -DPCZ because in addition to the aforementioned benefits it may also enhance tumor contrast. Of note, back in the early 1990s, Wiener and colleagues used dendrimer-based MRI contrast agents for *in vivo* diagnostic imaging applications.⁹ They found that the dendrimer-based reagents exhibited blood pool properties as well as extraordinary relaxivity values when chelated gadolinium groups were attached to PAMAM dendrimers. Other studies have shown that dendrimer conjugates have good tumor specificities.¹⁰ Researchers also performed systematic biological evaluations of different generations of PAMAM and found that the lower generation PAMAM (below generation 4) displayed a higher accumulation in kidney while higher generation PAMAM (above generation 4) showed a higher accumulation in liver.¹¹ Saad et al. compared the imaging properties of a group of nanocarriers including polymers, dendrimers, and liposomes which are coupled with Cy5.5. It was found that PAMAM G4 dendrimer coupled dye Cy5.5 (G4-Cy5.5) accumulated in significant quantities in the kidney, liver, and spleen.¹² These studies highlight the possibility of using different generation of PAMAM dendrimers to prepare dual-modality Affibody probes, in order to achieve probes with different *in vivo* profiles.

Conclusions

Dendrimer-based dual-modality imaging probe ^{64}Cu -DPCZ was successfully synthesized and demonstrated good imaging characteristics such as a high tumor uptake, good tumor contrast, and high specificity. Along with favourable pharmacokinetic properties, ^{64}Cu -DPCZ shows promise as a PET and NIRF agent for tumor imaging.

The authors gratefully acknowledge the Office of Science (BER), U.S. Department of Energy (DE-SC0008397), National Cancer Institute (NCI) R01 CA128908-03, and NCI In Vivo Cellular Molecular Imaging Center (ICMIC) grant P50 CA114747. Moreover, this work was also supported by China National Key Research and Development Program "973 Project" (9732006CB933205) and Science and Technology Pillar Program of Jiangsu province (BE2010721).

Notes and references

- Department of Chemistry and Chemical Engineering, Southeast University, Nanjing, Jiangsu, 211189, PR China.
- Molecular Imaging Program at Stanford (MIPS), Bio-X Program, Department of Radiology, Stanford University, California, 94305-5344 Tel: 650-723-7866; Fax: 650-736-7925; E-mail: zcheng@stanford.edu.

Electronic Supplementary Information (ESI) available: [Materials, experimental details, characterization data, biological assays]. See DOI: 10.1039/c000000x/

- Löfblom, J. Feldwisch, V. Tolmachev, J. Carlsson, S. Ståhl, F. Y. Frejd, *FEBS Lett.*, 2010, **584**, 2670; Z. Miao, J. Levi, Z. Cheng, *Amino Acids.*, 2011, **41**, 1037; J. Capala, K. Bouchelouche, *Curr. Opin. Oncol.*, 2010, **22**, 559.
- S. Trousil, S. Hoppmann, O. D. Nguyen, M. Kaliszczak, G. Tomasi, P. Iveson, D. Hiscock, E. O. Aboagye, *Clin. Cancer Res.*, 2014, **20**, 1632; M. Glaser, P. Iveson, S. Hoppmann, B. Indrevoll, A. Wilson, J. Arukwe, A. Danikas, R. Bhalla, D. Hiscock, *J. Nucl. Med.*, 2013, **54**, 1981; M. Satpathy, L. Wang, R. Zielinski, W. Qian, M. Lipowska, J. Capala, G. Y. Lee, H. Xu, Y. A. Wang, H. Mao, L. Yang, *Small*, 2014, **10**, 544; M. Yang, K. Cheng, S. Qi, H. Liu, Y. Jiang, H. Jiang, J. Li, K. Chen, H. Zhang, Z. Cheng, *Biomaterials*, 2013, **34**, 2796; S. Qi, Z. Miao, H. Liu, Y. Xu, Y. Feng, Z. Cheng, *Bioconjug. Chem.*, 2012, **23**, 1149; A. Perols, H. Honarvar, J. Strand, R. Selvaraju, A. Orlova, A. E. Karlström, V. Tolmachev, *Bioconjug. Chem.*, 2012, **23**, 1661. J. Gao, K. Chen, Z. Miao, G. Ren, X. Chen, S. S. Gambhir, Z. Cheng, *Biomaterials*, 2011, **32**, 2141.
- M. M. Moasser, *Oncogene*, 2007, **26**, 6469; J. Carlsson, H. Nordgren, J. Sjöström, K. Wester, K. Villman, N. O. Bengtsson, B. Ostenstad, H. Lundqvist, C. Blomqvist, *Br. J. Cancer*, 2004, **90**, 2344.
- K. Cheng, Z. Cheng, *Curr. Med. Chem.*, 2012, **19**, 4767; J. A. Moss, A. L. Våvere, A. Azhdarinia, *Curr. Med. Chem.*, 2012, **19**, 3255; A. Azhdarinia, P. Ghosh, S. Ghosh, N. Wilganowski, E. M. Sevic-Muraca, *Mol. Imaging Biol.*, 2012, **14**, 261.
- D. A. Tomalia, L. A. Reyna, S. Svenson, *Biochem. Soc. Trans.*, 2007, **35**, 61; H. Kobayashi, M. W. Brechbiel, *Mol. Imaging*, 2003, **2**, 1.
- T. J. Wadas, E. H. Wong, G. R. Weisman, C. J. Anderson, *Curr. Pharm. Des.*, 2007, **13**, 3; C. A. Boswell, X. Sun, W. Niu, G. R. Weisman, E. H. Wong, A. L. Rheingold, C. J. Anderson, *J. Med. Chem.*, 2004, **47**, 1465; Z. Cheng, Z. Xiong, M. Subbarayan, X. Chen, S. S. Gambhir, *Bioconjug. Chem.*, 2007, **18**, 765.
- C. L. Ferreira, D. T. T. Yapp, S. Crisp, B. W. Sutherland, S. S. W. Ng, M. Gleave, C. Bensimon, P. Jurek, G. E. Kiefer, *Eur. J. Nucl. Med. Mol. Imaging*, 2010, **37**, 2117; E. Mume, A. Asad, N. M. Di Bartolo, L. Kong, C. Smith, A. M. Sargeson, R. Price, S. V. Smith, *Dalton Trans.*, 2013, **42**, 14402; E. W. Price, C. Orvig, *Chem. Soc. Rev.*, 2014, **43**, 260.
- A. Orlova, M. Magnusson, T. L. Eriksson, M. Nilsson, B. Larsson, I. Höiden-Guthenberg, C. Widström, J. Carlsson, V. Tolmachev, S. Ståhl, F. Y. Nilsson, *Cancer Res.*, 2006, **66**, 4339; M. A. Fortin, A. Orlova, P. U. Malmström, V. Tolmachev, *Int. J. Mol. Med.*, 2007, **19**, 285.
- E. C. Wiener, M. W. Brechbiel, H. Brothers, R. L. Magin, O. A. Gansow, D. A. Tomalia, P. C. Lauterbur, *Magn. Reson. Med.*, 1994, **31**, 1.
- N. Malik, R. Wiwattanapatapee, R. Klopsch, K. Lorenz, H. Frey, J. W. Weener, E. W. Meijer, W. Paulus, R. Duncan, *J. Control Release*, 2000, **65**, 133; S. D. Konda, S. Wang, M. Brechbiel, E. C. Wiener, *Invest. Radiol.*, 2002, **37**, 199.
- J. C. Roberts, M. K. Bhalgat, R. T. Zera, *J. Biomed. Mater. Res.*, 1996, **30**, 53; H. Kobayashi, M. W. Brechbiel, *Adv. Drug Deliv. Rev.*, 2005, **57**, 2271.
- M. Saad, O. B. Garbuzenko, E. Ber, P. Chandna, J. J. Khandare, V. P. Pozharov, T. Minko, *J. Control. Release*, 2008, **130**, 107.